

PAPER • OPEN ACCESS

Broadband control on scattering events with interferometric coherent waves

To cite this article: Jeng Yi Lee *et al* 2021 *New J. Phys.* **23** 063014

View the [article online](#) for updates and enhancements.



PAPER

Broadband control on scattering events with interferometric coherent waves

OPEN ACCESS

RECEIVED

20 February 2021

REVISED

20 April 2021

ACCEPTED FOR PUBLICATION

10 May 2021

PUBLISHED

8 June 2021

Original content from
this work may be used
under the terms of the
[Creative Commons
Attribution 4.0 licence](#).

Any further distribution
of this work must
maintain attribution to
the author(s) and the
title of the work, journal
citation and DOI.



Jeng Yi Lee^{1,*} , Lujun Huang², Lei Xu³ , Andrey E Miroshnichenko²  and
Ray-Kuang Lee^{4,5,*} 

¹ Department of Opto-Electronic Engineering, National Dong Hwa University, Hualien 974301, Taiwan

² School of Engineering and Information Technology, University of New South Wales, Canberra ACT 2600, Australia

³ Advanced Optics and Photonics Laboratory, Department of Engineering, School of Science and Technology, Nottingham Trent University, Nottingham, United Kingdom

⁴ Institute of Photonics Technologies, National Tsing Hua University, Hsinchu 300, Taiwan

⁵ Physics Division, National Center for Theoretical Science, Taipei 10617, Taiwan

* Author to whom any correspondence should be addressed.

E-mail: jengyilee@gms.ndhu.edu.tw and rklee@ee.nthu.edu.tw

Keywords: Mie-scattering, broadband control, coherent wave interferences

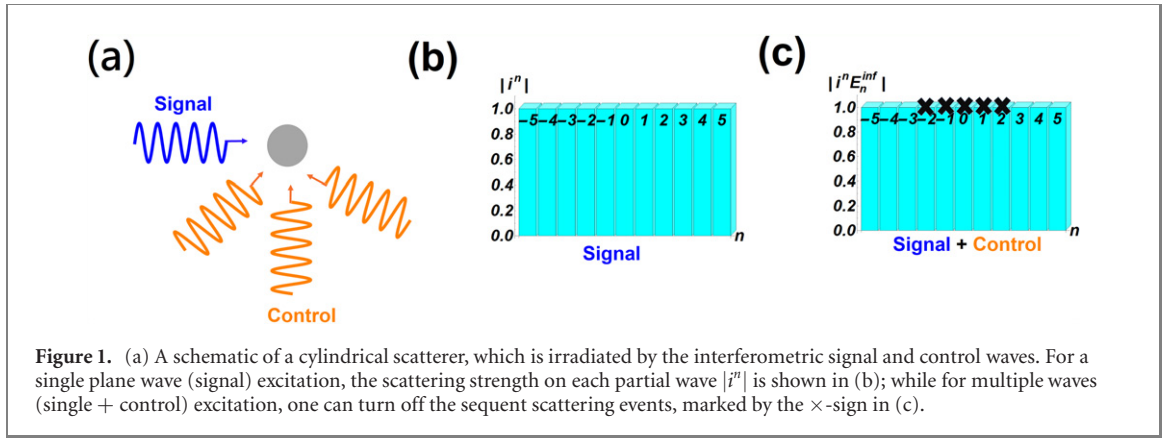
Abstract

We propose a universal strategy to realize a broadband control on arbitrary scatterers, through multiple coherent beams. By engineering the phases and amplitudes of incident beams, one can suppress the dominant scattering partial waves, making the obstacle lose its intrinsic responses in a broadband spectrum. The associated coherent beams generate a finite and static region, inside which the corresponding electric field intensity and Poynting vector vanish. As a solution to go beyond the sum-rule limit, our methodology is also irrespective of inherent system properties, as well as extrinsic operating wavelength, providing a non-invasive control on the wave-obstacles interaction for any kinds of shape.

1. Introduction

Making functional sub-wavelength scatterers has been attractive for a variety of applications, such as superdirective scatterers [1–3], perfect absorption objects [4, 5], magnetic resonator based devices [6–8], Kerker effect and beyond [9–11], anapole [12], and superscattered objects [13, 14]. In particular, to have invisible cloaks, the concepts of transformation optics [15, 16] and scattering cancellation method [17–19] have been applied not only to electromagnetic waves, but also to acoustic [20–24] and water waves [25, 26], thermal diffusion science [27–29], quantum matter waves [30–34], and elastic wave in solids [35–37]. However, for these methods and the consequently improved efforts [38], we still suffer from the superluminal propagation [39, 40], and limited operating bandwidth imposed by Kramers–Kronig relation [41, 42]. To manipulate light-obstacles interaction in nanoscales, it is still desirable to have a non-invasive and efficient way to have objects working in a broadband spectrum.

As pointed out by Purcell [43], the integration of the extinction cross section over all the spectra is related to the static electric and magnetic material parameters, leading to the sum-rule limit. Therefore, under a plane wave excitation, no scattering systems can remain stationary scattering responses in a broadband spectrum. In this paper, we demonstrate that it is possible to turn off or amplify the target scattering partial waves with interferometric coherent waves. With a proper setting on the phases and intensities, destructive interferometry on the dominant partial waves can be achieved, resulting in an arbitrary object invisible. At the same time, a finite and static region emerges, inside which the electric field and the corresponding Poynting vector almost completely vanish. Counter-intuitively, when the system contains high-order scattering partial waves, the overall scattering would be amplified even its physical size is much smaller than this zero field region. Moreover, the operating wavelength for such a destructive removal of excitation exists for a broadband spectrum, overcoming the fundamental sum-rule limit obtained from a single plane wave excitation. There exist more than one settings for the interferometric



field in the excitation, demonstrating the flexibility for experimental implementations. The robustness of our methodology on invisibility is also verified by introducing the deviations in the scatter displacements, intensities and illumination angles of incident beams, and different shapes of systems. Our results pave an alternative route to manipulate waves and obstacles in the extremely small scale.

2. Theoretical analysis

Without loss of generality, we consider the illumination waves composed by a set of plane waves on a cylindrical scatterer, as illustrated in figure 1(a). Here, the symmetrical axis of the cylindrical axis is chosen as the z -axis. For a single plane wave of s -polarized electric field propagating in x -axis, it can be described as $E_1 \hat{z} e^{ik_0 r \cos \theta}$ with the signal wave denoted by E_1 , the environmental wavenumber k_0 , and the azimuthal angle θ . By a combination of proper eigenstates $\nu_n(\vec{r})$, which rely on the scatterer structures, we have $E_1 \hat{z} e^{ik_0 r \cos \theta} = \hat{z} E_1 \sum_n \phi_n \nu_n(\vec{r})$, with a complex coefficient ϕ_n . The time dependence for each plane wave has the form $e^{-i\omega t}$. As an example for the cylindrical scatter, we adopt the Bessel and the first kind of Hankel functions obeying the Helmholtz equation for the eigenstates, i.e., $J_n(k_0 r) e^{in\theta}$ and $H_n^{(1)}(k_0 r) e^{in\theta}$, respectively. Then, the incident wave, denoted as *signal*, can be expressed as $E_1 \hat{z} e^{ik_0 r \cos \theta} = E_1 \hat{z} \sum_{n=-\infty}^{\infty} i^n J_n(k_0 r) e^{in\theta}$, here the index, n , represents a series of partial waves [44]. The associated scattering wave generated by the scatterer has the form $\vec{E}_{sc} = E_1 \hat{z} \sum_{n=-\infty}^{\infty} i^n a_n^s H_n^{(1)}(k_0 r) e^{in\theta}$, with the complex scattering coefficient a_n^s .

For signal plane wave, the resulting excitation strength for this cylinder can be expressed by $|i^n|$, i.e.,

$$\text{excitation of signal wave : } |i^n|, \quad (1)$$

as shown in figure 1(b).

To describe the total illumination and scattering waves, one has $\vec{E}_{in} = \hat{z} \sum_{n=-\infty}^{\infty} i^n J_n(k_0 r) e^{in\theta} E_n^{inf}$ and $\vec{E}_{sc} = \hat{z} \sum_{n=-\infty}^{\infty} i^n E_n^{inf} e^{in\theta} H_n^{(1)}(k_0 r) a_n^s$, with the introduction of an interfering factor E_n^{inf} , which has the form

$$E_n^{inf} = E_1 + \sum_{m=2}^{m=s} e^{-in\Phi_m} E_m. \quad (2)$$

Here, the first term in the right-handed side of equation (2) corresponds to the signal wave; while the others represent $s - 1$ ($s \geq 2$) control waves whose complex wave amplitudes and incident angle are defined as E_m and Φ_m , respectively.

Now the total excitation strengths from signal and control waves would become $|i^n E_n^{inf}|$, i.e.,

$$\text{excitation of signal + control waves : } |i^n E_n^{inf}|, \quad (3)$$

as shown in figure 1(c). As we are going to illustrate, our target is to demonstrate that the irradiation from a proper setting of signal and control waves can turn off the initially excitation sources, as illustrated in figure 1(c), resulting in scatterers lose their functionality. The corresponding scattering and absorption powers are $P_{sc} = 2/k_0 \times \sqrt{\epsilon_0/\mu_0} \sum_{n=-\infty}^{\infty} |E_n^{inf}|^2 |a_n^s|^2$ and $P_{abs} = -2/k_0 \times \sqrt{\epsilon_0/\mu_0} \sum_{n=-\infty}^{\infty} |E_n^{inf}|^2 [\text{Re}(a_n^s) + |a_n^s|^2]$, with the environmental permittivity and permeability denoted as ϵ_0 and μ_0 , respectively [45].

Now, suppose that our scattering system has $2N + 1$ dominant partial waves (scattering channels). The only way to eliminate the scattering of these dominant partial waves is to produce the destructive interference of these target channels, i.e., $E_n^{inf} = 0$ from $n = [-N, N]$. However, employing the results from reference [45] directly leads to zeros in the excitation waves. New strategy is needed to achieve invisibility.

To obtain a non-trivial solution, one possibility is to expand the amount of control waves to $2N + 1$ in total at least. Then, we have the following $2N + 1$ equations to be satisfied:

$$E_1 + \sum_{m=2}^{2N+2} e^{-im\Phi_m} E_m = 0, \quad \text{for } n = [-2N, 2N]. \quad (4)$$

Here, in each equation there are three degrees of freedom for the extrinsic control parameters: intensity and phase of a control wave E_i , and the corresponding incident angle Φ_i . In general, one should have a variety of solutions to satisfy the necessary condition in equation (4).

3. Results and discussion

To demonstrate our control on the scattering events, a lossless silicon-embedded system is considered, with a high refractive index $\epsilon_1 = 12$ and the radius $a = 0.18\lambda$. λ is incident wavelength. Here, we tackle the first five dominant scattering channels, as shown in figure 2(a). These five scattering events correspond to the electric dipole ($n = 0$), magnetic dipole ($n \pm 1$), and magnetic quadrupole ($n \pm 2$). The corresponding far-field scattering distribution and the intensity of the electric field are illustrated in figures 2(b) and (c) for a single wave excitation (signal only). Details on how to obtain the far-field scattering distribution are provided in Supplementary Materials. Now, in order to suppress these five dominant scattering partial waves, we construct an illumination system with another five control waves, denoted as $(E_2, E_3, E_4, E_5, E_6)$, with the corresponding incident angles $(\Phi_2, \Phi_3, \Phi_4, \Phi_5, \Phi_6)$. Then, we rewrite equation (4) into the following matrix presentation:

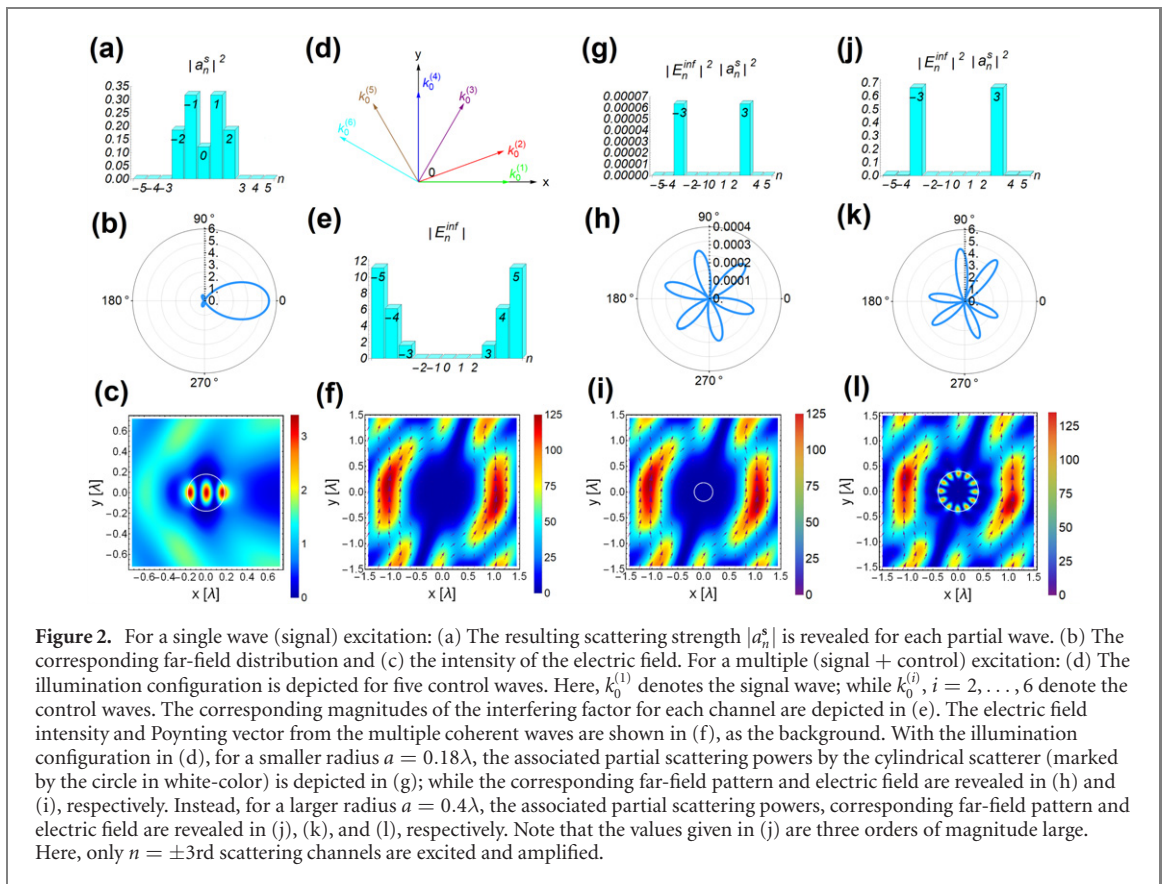
$$\begin{bmatrix} -1 \\ -1 \\ -1 \\ -1 \\ -1 \end{bmatrix} = \begin{bmatrix} e^{-2i\Phi_2} & e^{-2i\Phi_3} & e^{-2i\Phi_4} & e^{-2i\Phi_5} & e^{-2i\Phi_6} \\ e^{-i\Phi_2} & e^{-i\Phi_3} & e^{-i\Phi_4} & e^{-i\Phi_5} & e^{-i\Phi_6} \\ 1 & 1 & 1 & 1 & 1 \\ e^{i\Phi_2} & e^{i\Phi_3} & e^{i\Phi_4} & e^{i\Phi_5} & e^{i\Phi_6} \\ e^{2i\Phi_2} & e^{2i\Phi_3} & e^{2i\Phi_4} & e^{2i\Phi_5} & e^{2i\Phi_6} \end{bmatrix} \begin{bmatrix} E_2 \\ E_3 \\ E_4 \\ E_5 \\ E_6 \end{bmatrix}. \quad (5)$$

Here, we set $E_1 = 1$. Figure 2(d) shows illumination angles by $[\Phi_2 = \pi/9, \Phi_3 = \pi/3, \Phi_4 = \pi/2, \Phi_5 = 2\pi/3, \Phi_6 = 5\pi/6]$, with control wave amplitudes $[E_2 = -2.17, E_3 = 3.28, E_4 = -3.78, E_5 = 2.31, E_6 = -0.64]$ obtained by solving equation (3). In principle, one can set the incident angles arbitrarily and find out the corresponding complex amplitudes by equation (3). With these obtained results, we analyze the interfering factors for each excited scattering events, as shown in figure 2(e). As one can see, a complete destructive interference condition happens for the target channels $n = [-2, -1, 0, 1, 2]$, with all the zero values. Meanwhile, non-zero interfering factors emerge on non-target scattering channels, i.e., $n = \pm 3, \pm 4$, and ± 5 . This result indicates that when the destructive interferometry applies to the dominant scattering channels, one can completely suppress the scattering events at the price that the originally non-dominant scattering channels are amplified. In figure 2(f), we show the background fields and Poynting vectors without our scatterer.

In figure 2(g), we reveal the suppressed scattering on our system when embedding illumination configurations of figure 2(d). One can easily see that the corresponding far-field scattering pattern shown in figure 2(h) is significantly suppressed, i.e., at least three orders of magnitude smaller. The resulting electric field, as well as the time-averaged Poynting vectors, shown in figure 2(i) clearly demonstrate that the energy bypasses scatterer in the central region. Moreover, a finite and static region emerge within $x = [-0.5\lambda, 0.5\lambda]$ and $y = [-0.5\lambda, 0.5\lambda]$, inside which nearly all the intensity and energy Poynting vectors vanish. With the comparison between figures 2(f) and (i), it is almost indistinguishable both for the field distribution and Poynting vectors, supporting the realization of invisibility.

At a quick glance, as the existence of a finite and static region induced by the multiple wave excitation, one may contribute it for the reason to make the scatterer lose its functionality, as the physical size of our scatterers is smaller than the size of this zero-field region. As shown in figure 2(e), even though the interfering factors are completely suppressed for $n = [-2, -1, 0, 1, 2]$, other channels still survive and amplified. To highlight the this effect, we choose a bigger scatterer by changing the radius of our cylinder from $a = 0.18\lambda$ to $a = 0.4\lambda$. With the same setting in figure 2(d), now, the resulting scattering events are enhanced for the $n = \pm 3$ rd scattering channels, as shown in figure 2(j). Nevertheless, far-field scattering pattern and field intensity (also the Poynting vector) are shown in figures 2(k) and (l), respectively, which the invisibility is broken.

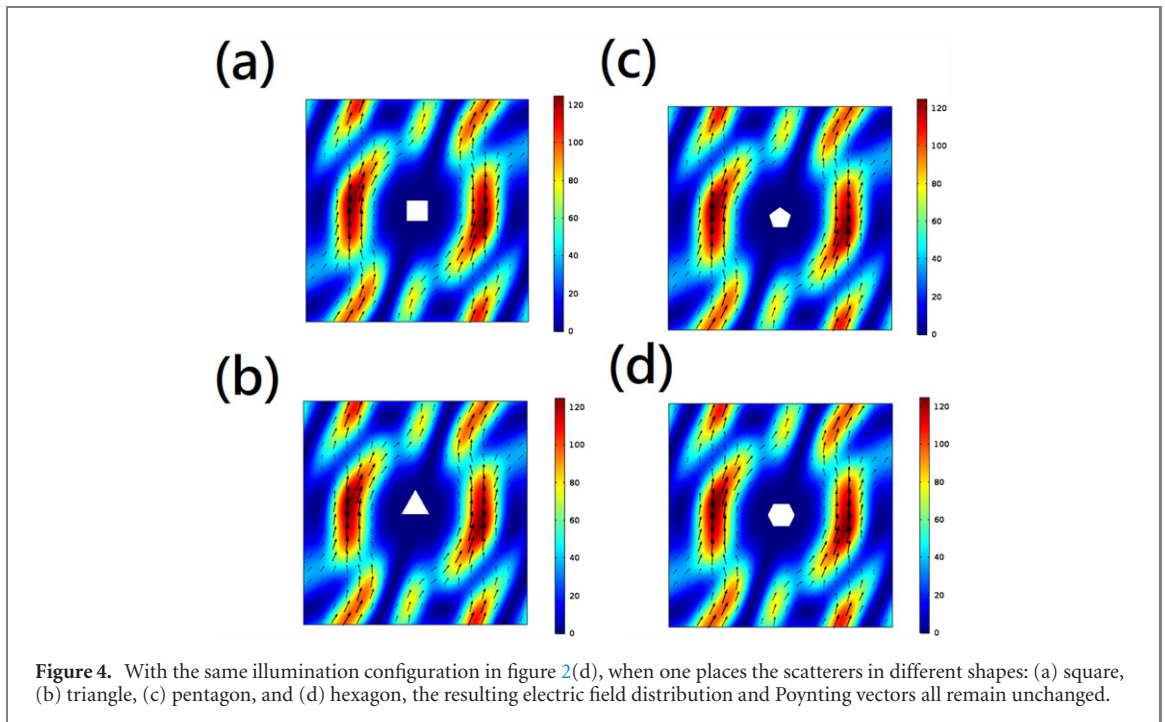
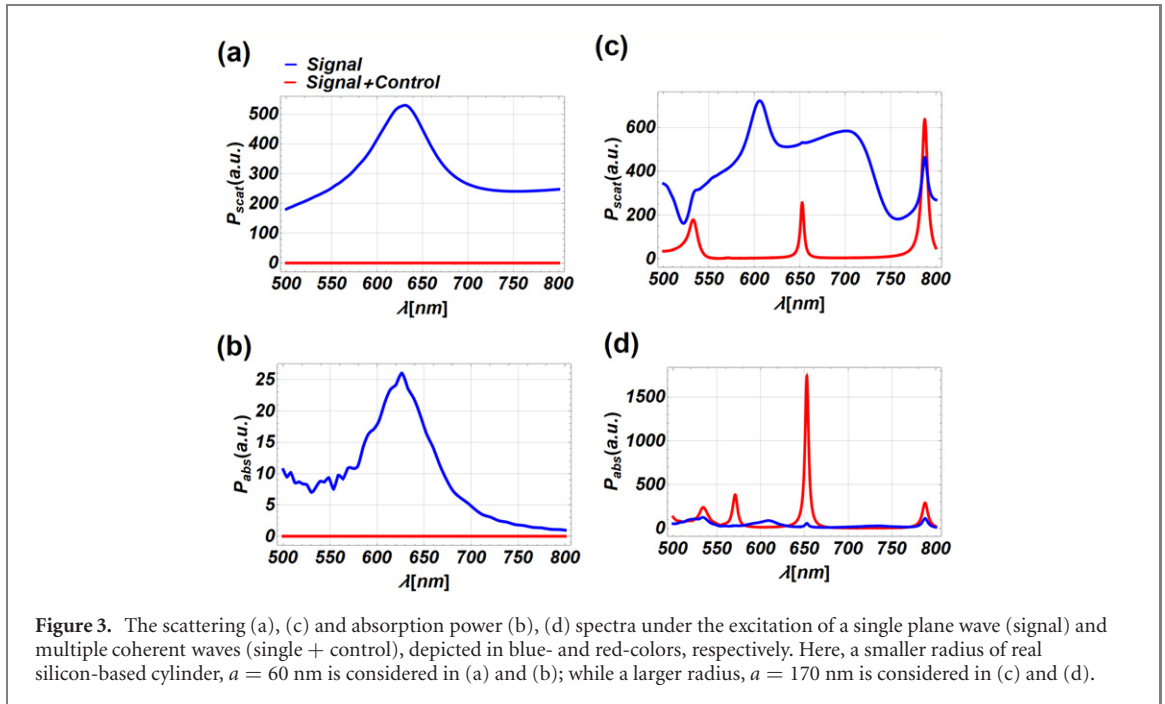
Instead of using a structured wave to select the multipolar modes [45–48], our goal in this work with multiple wave excitation is entirely different. The related methods developed in references [45–48] can not



be implemented in designing invisibility. Moreover, these selective modes are highly sensitive to the distribution of phases and amplitudes in spatial location. Below, we will demonstrate that this invisible structured waves can allow deviations in scatter displacements, intensities, illumination direction, and scatter shapes. Furthermore, our methodology can support extreme broadband control through the interferometric coherent waves. If we keep all the system parameters fixed, including the illumination angles, intensities and phases of control waves, but only tune the incident wavelength. In figures 3(a) and (b), we choose the real silicon-based cylinder which its dispersion relation is based on experimental data [49], with the radius $a = 60$ nm and scan the incident wavelength from 500 to 800 nm. Interestingly, compared to the plane wave excitation, depicted in blue-color, by multiple wave excitation, both the scattering and absorption power spectra give us the zero values in this wavelength range, as depicted in red-color. Even though it is known that for any invisible cloak illuminated by a single plane wave, Kramers–Kronig relation and sum-rule limit prevent the realization of a broadband operation. Our results demonstrate the scenario to go beyond the sum-rule limit, indicating the scatterer system working at this wavelength window with lowest-orders in the partial scattering waves.

For a larger size silicon cylinder, in figures 3(c) and (d), we choose $a = 170$ nm as an example. Even though such a larger size system can support higher-order scattering channels, the target scattering events can remain suppressed with a multiple wave excitation. As a guideline, one solution to further suppress these higher-order scattering channels is to introduce more control waves.

As for the influences on the invisibility from the mismatches in intensities and illumination angles of incident beams, as well as the scatterer displacement (with the help of Graft's addition theorem [50]), a detailed analysis is presented in supplementary materials. Our finding reveals that the interferometric method is robust to allow these mismatching, offering flexibility toward the experimental implementation. For different kinds of shape, we also studied scatterers in the shape of a square, triangle, hexagon, and a pentagon, by Comsol, as shown in figure 4. All of our outcomes can support invisibility. Even though the analysis in this work is demonstrated for the two-dimensional system, but it is readily applied to a three-dimensional scatterer or clusters. Last but not least, as shown in figures 2(j)–(l), we note that the crucial role to achieve invisibility is based on the total number of dominant scattering partial waves, but not on the specific value of scattering coefficients.



4. Conclusion

In summary, we have demonstrated a novel way by extrinsically imposing interferometric multiple waves to manage the excitation of partial waves. Compared to the single plane wave illumination, we reveal the possibility to support invisibility or to enhance target scattering partial waves, irrespective of internal system configuration. Unlike the known wave-obstacle interaction, which strongly relies on the material dispersion, such a multiple wave illumination provides a non-invasion way to avoid this physical constraint. It is the interferometric coherent waves, to support the existence of stationary scattering response for a broadband wavelength, beyond the sum-rule limit. The coherent control paves a new and exciting way to manipulate wave-obstacle interaction in the deep subwavelength scale for a variety of waves physics.

Acknowledgment

This work is supported by Ministry of Science and Technology, Taiwan (107-2112-M-259-007-MY3 and 109-2112-M-007-019-MY3). The work of AEM was supported by the Australian Research Council and UNSW Scientia Fellowship.

Data availability statement

All data that support the findings of this study are included within the article (and any supplementary files).

ORCID iDs

Jeng Yi Lee  <https://orcid.org/0000-0003-1168-7867>

Lei Xu  <https://orcid.org/0000-0001-9071-4311>

Andrey E Miroshnichenko  <https://orcid.org/0000-0001-9607-6621>

Ray-Kuang Lee  <https://orcid.org/0000-0002-7171-7274>

References

- [1] Arslanagić S and Ziolkowski R W 2018 Highly subwavelength, superdirective cylindrical nanoantenna *Phys. Rev. Lett.* **120** 237401
- [2] Liu W, Miroshnichenko A E, Neshev D N and Kivshar Y S 2012 Broadband unidirectional scattering by magneto-electric core-shell nanoparticles *ACS Nano* **6** 5489–97
- [3] Hancu I M, Curto A G, Castro-López M, Kuttge M and van Hulst N F 2014 Multipolar interference for directed light emission *Nano Lett.* **14** 166–71
- [4] Noh H, Chong Y, Stone A D and Cao H 2012 Perfect coupling of light to surface plasmons by coherent absorption *Phys. Rev. Lett.* **108** 186805
- [5] Bai P, Wu Y and Lai Y 2016 Multi-channel coherent perfect absorbers *Europhys. Lett.* **114** 28003
- [6] Schuller J A, Zia R, Taubner T and Brongersma M L 2007 Dielectric metamaterials based on electric and magnetic resonances of silicon carbide particles *Phys. Rev. Lett.* **99** 107401
- [7] Feng T, Xu Y, Zhang W and Miroshnichenko A E 2017 Ideal magnetic dipole scattering *Phys. Rev. Lett.* **118** 173901
- [8] Liu W 2017 Generalized magnetic mirrors *Phys. Rev. Lett.* **119** 123902
- [9] Lee J Y, Miroshnichenko A E and Lee R-K 2017 Reexamination of Kerker's conditions by means of the phase diagram *Phys. Rev. A* **96** 043846
- [10] Lee J Y, Miroshnichenko A E and Lee R-K 2018 Simultaneously nearly zero forward and nearly zero backward scattering objects *Opt. Express* **26** 30393–9
- [11] Liu W and Kivshar Y S 2018 Generalized Kerker effects in nanophotonics and meta-optics [Invited] *Opt. Express* **26** 13085–105
- [12] Miroshnichenko A E, Evlyukhin A B, Yu Y F, Bakker R M, Chipouline A, Kuznetsov A I, Luk'yanchuk B, Chichkov B N and Kivshar Y S 2015 Nonradiating anapole modes in dielectric nanoparticles *Nat. Commun.* **6** 1–8
- [13] Ruan Z and Fan S 2010 Superscattering of light from subwavelength nanostructures *Phys. Rev. Lett.* **105** 013901
- [14] Qian C, Lin X, Yang Y, Xiong X, Wang H, Li E, Kaminer I, Zhang B and Chen H 2019 Experimental observation of superscattering *Phys. Rev. Lett.* **122** 063901
- [15] Pendry J B, Schurig D and Smith D R 2006 Controlling electromagnetic fields *science* **312** 1780–2
- [16] Leonhardt U 2006 Optical conformal mapping *science* **312** 1777–80
- [17] Kerker M 1975 Invisible bodies *J. Opt. Soc. Am.* **65** 376–9
- [18] Alù A and Engheta N 2005 Achieving transparency with plasmonic and metamaterial coatings *Phys. Rev. E* **72** 016623
- [19] Alù A and Engheta N 2007 Plasmonic materials in transparency and cloaking problems: mechanism, robustness, and physical insights *Opt. Express* **15** 3318–32
- [20] Cummer S A and Schurig D 2007 One path to acoustic cloaking *New J. Phys.* **9** 45
- [21] Zhang S, Xia C and Fang N 2011 Broadband acoustic cloak for ultrasound waves *Phys. Rev. Lett.* **106** 024301
- [22] Cummer S A, Popa B-I, Schurig D, Smith D R, Pendry J, Rahm M and Starr A 2008 Scattering theory derivation of a 3D acoustic cloaking shell *Phys. Rev. Lett.* **100** 024301
- [23] Guild M D, Alù A and Haberman M R 2011 Cancellation of acoustic scattering from an elastic sphere *J. Acous. Soc. Am.* **129** 1355–65
- [24] Sanchis L, García-Chocano V M, Llopis-Pontiveros R, Climente A, Martínez-Pastor J, Cervera F and Sánchez-Dehesa J 2013 Three-dimensional axisymmetric cloak based on the cancellation of acoustic scattering from a sphere *Phys. Rev. Lett.* **110** 124301
- [25] Farhat M, Enoch S, Guenneau S and Movchan A 2008 Broadband cylindrical acoustic cloak for linear surface waves in a fluid *Phys. Rev. Lett.* **101** 134501
- [26] Urzhumov Y A and Smith D R 2011 Fluid flow control with transformation media *Phys. Rev. Lett.* **107** 074501
- [27] Schittny R, Kadic M, Guenneau S and Wegener M 2013 Experiments on transformation thermodynamics: molding the flow of heat *Phys. Rev. Lett.* **110** 195901
- [28] Guenneau S, Amra C and Veynante D 2012 Transformation thermodynamics: cloaking and concentrating heat flux *Opt. Express* **20** 8207–18
- [29] Farhat M, Chen P-Y, Bagci H, Amra C, Guenneau S and Alù A 2015 Thermal invisibility based on scattering cancellation and mantle cloaking *Sci. Rep.* **5** 1–9
- [30] Zhang S, Genov D A, Sun C and Zhang X 2008 Cloaking of matter waves *Phys. Rev. Lett.* **100** 123002
- [31] Lin D-H 2010 Cloaking spin-1/2 matter waves *Phys. Rev. A* **81** 063640
- [32] Lin D-H 2011 Cloaking two-dimensional fermions *Phys. Rev. A* **84** 033624

- [33] Lee J Y and Lee R-K 2014 Hiding the interior region of core-shell nanoparticles with quantum invisible cloaks *Phys. Rev. B* **89** 155425
- [34] Liao B, Zebarjadi M, Esfarjani K and Chen G 2012 Cloaking core-shell nanoparticles from conducting electrons in solids *Phys. Rev. Lett.* **109** 126806
- [35] Stenger N, Wilhelm M and Wegener M 2012 Experiments on elastic cloaking in thin plates *Phys. Rev. Lett.* **108** 014301
- [36] Farhat M, Guenneau S and Enoch S 2009 Ultrabroadband elastic cloaking in thin plates *Phys. Rev. Lett.* **103** 024301
- [37] Farhat M, Guenneau S, Enoch S and Movchan A B 2009 Cloaking bending waves propagating in thin elastic plates *Phys. Rev. B* **79** 033102
- [38] Li J and Pendry J B 2008 Hiding under the carpet: a new strategy for cloaking *Phys. Rev. Lett.* **101** 203901
- [39] Miller D A B 2006 On perfect cloaking *Opt. Express* **14** 12457–66
- [40] Zhang B 2012 Electrodynamics of transformation-based invisibility cloaking *Light Sci. Appl.* **1** e32
- [41] Fleury R, Monticone F and Alu A 2015 Invisibility and cloaking: origins, present, and future perspectives *Phys. Rev. Appl.* **4** 037001
- [42] Monticone F and Alu A 2013 Do cloaked objects really scatter less? *Phys. Rev. X* **3** 041005
- [43] Purcell E M 1969 On the absorption and emission of light by interstellar grains *Astrophys. J.* **158** 433
- [44] Bohren C F and Huffman D R 2008 *Absorption and Scattering of Light by Small Particles* (New York: Wiley)
- [45] Lee J Y, Chung Y-H, Miroshnichenko A E and Lee R-K 2019 Linear control of light scattering with multiple coherent waves excitation *Opt. Lett.* **44** 5310–3
- [46] Xi Z and Urbach H 2017 Magnetic dipole scattering from metallic nanowire for ultrasensitive deflection sensing *Phys. Rev. Lett.* **119** 053902
- [47] Das T, Iyer P P, DeCrescent R A and Schuller J A 2015 Beam engineering for selective and enhanced coupling to multipolar resonances *Phys. Rev. B* **92** 241110
- [48] Wei L, Zayats A V and Rodríguez-Fortuño F J 2018 Interferometric evanescent wave excitation of a nanoantenna for ultrasensitive displacement and phase metrology *Phys. Rev. Lett.* **121** 193901
- [49] Palik E D 1998 *Handbook of Optical Constants of Solids* vol 3 (New York: Academic)
- [50] Kristensen P T, Lodahl P and Mørk J 2010 Light propagation in finite-sized photonic crystals: multiple scattering using an electric field integral equation *J. Opt. Soc. Am. B* **27** 228–37